CR-66095

EVALUATION OF THE USE OF OCCULTATION DATA IN DIFFERENTIAL CORRECTION PROCEDURES FOR DETERMINATION OF THE LUNAR ORBIT

By D. H. Lewis

Prepared under Contract No. NAS 1-4605-3 by
TRW Systems
One Space Park, Redondo Beach,
California

for

NATIONAL AERONAUTICS AND SPACE ADMINISTRATION

NASA CR- 66095

EVALUATION OF THE USE OF OCCULTATION DATA IN DIFFERENTIAL CORRECTION PROCEDURES FOR DETERMINATION OF THE LUNAR ORBIT

By D. H. Lewis

Prepared under Contract No. NAS 1-4605-3 by
TRW Systems
One Space Park, Redondo Beach,
California

for

NATIONAL AERONAUTICS AND SPACE ADMINISTRATION

ABSTRACT

This report is a description of a study conducted to evaluate occultation times as an aid to convergence in the differential correction of lunar satellite orbits. Occultations of the earth and the sun were considered, in combination with range and range-rate data from the Deep Space Network stations at Goldstone, California; Woomera, Australia; and Madrid, Spain.

CONTENTS

ILLUSTRATIONS

TABLES

SYMBOLS

a_m	radius of moon
$\bar{R}$	geocentric position vector of observer
$\bar{R}_m$	geocentric position vector of moon
$\bar{R}_s$	geocentric position vector of sun
w_i^s	meridian plane coordinates of observing station
$\bar{x}$	geocentric position vector of vehicle
$\bar{y}$	ray from observer to vehicle
α_i	right ascension of observing station at time t_i
$\bar{\gamma}$	earth occultation function: position of moon relative to observer; sun occultation function: position of observer relative to moon
ρ	earth occultation function: distance from observer to moon's limb; sun occultation function: distance from vehicle to moon's limb
σ_t	uncertainty (one sigma) in measurement of occultation times
σ_ϕ	uncertainty (one sigma) in occultation function corresponding to σ_t
ϕ	occultation function, $(\bar{\gamma}^T\bar{\psi}/\lvert\psi\rvert) - \sqrt{\rho}$
$\bar{\omega}$	earth's rotational velocity vector
$\bar{\psi}$	earth occultation function: position of vehicle relative to observer; sun occultation function: position of observer relative to vehicle

EVALUATION OF THE USE OF OCCULTATION DATA IN DIFFERENTIAL CORRECTION PROCEDURES FOR DETERMINATION OF THE LUNAR ORBIT

By D. H. Lewis

1. SUMMARY

This study has been conducted to evaluate occultation times as an aid to convergence and to reduction of the final uncertainties in the converged result for differential correction of lunar satellite orbits. Occultations of the earth and the sun (as seen from a lunar satellite) were considered; the measurement of the time of earth occultation was assumed to have a standard deviation of 0.5 second, for sun occultation measurements, the standard deviation was 0.7 second.

Occultation data were found not to be useful as a convergence aid because of extraneous zeros in the occultation function. When large energy errors were present in the initial orbital estimates, the actual occultation time could be closer to an extraneous zero than to its respective zero, and would result in an inappropriate residual and correction. Hence, occultations were of greatest value when the solution was already closely approximated and when convergence problems were not prevalent.

Occultation data of nominal quality, (σ_t = 0.5 and 0.7 seconds on earth and sun occultations, respectively) only slightly reduce the uncertainties in the converged state vector, when used with the standard (two station, one $\rho,\dot{\rho}$ set perminute) observation schedule. Substantial reduction in these uncertainties was obtained, however, for occultation data one order of magnitude better than nominal.

When used with very short data arcs (less than 15 minutes), the nominal quality occultation was found to be effective in reducing state vector uncertainties, especially in the velocity components, where an order of magnitude reduction was noted.

2. INTRODUCTION

Occultation times give information about orbital period, i.e., they indicate the times at which the lunar satellite has a given position. The possibility of their use as an aid to convergence, where large energy errors may be expected, is of interest. In addition, the high accuracy with which the time of occultation can be measured gives it potential as a means of reducing the uncertainties in the converged result of a differential correction based initially on range and range-rate data only.

Two types of occultations are considered; they are designated earth occultations and sun occultations. Earth occultations are obtained by noting at one of the Deep Space Network (DSN) stations the time of cutoff of the spacecraft telemetry signal. Sun occultations are obtained by monitoring the (telemetered) output of the spacecraft sun sensor; this is assumed to be a discrete event, and is independent of the earth-based tracking station taking the measurement. Measurements are assumed to have a standard deviation of 0.5 second for earth occultation and 0.7 second for sun occultation, with a bias of 3 seconds on both types.

The nominal LOPP observation schedule of one $\rho, \dot{\rho}$ set per minute from the DSN stations at Goldstone, Woomera, and Madrid was used for all test cases. Emersion times were included in the occultation data, with the same standard deviation as the immersion times, although the difficulties of reacquisition of the spacecraft as it comes out from behind the moon may result in data of somewhat lower quality.

3. MATHEMATICAL FORMULATION

3.1 Occultation Function

Occultation data are handled by introducing an occultation function which indicates when a ray from the observer to the vehicle is tangent to the moon. This function can be developed for earth occultations in the following manner (reference 1). Introduce the following geocentric position (column) vectors:

$\bar{x}$ = position of vehicle

$\bar{R}$ = position of observer

$\bar{R}_m$ = position of moon

Then a ray from the observer to the vehicle has the vector equation

$$\bar{y}(\tau) = \bar{R} + \tau(\bar{x} - \bar{R}) \tag{1}$$

i.e., a straight line with $\bar{y}(o) = \bar{R}$ and $\bar{y}(1) = x$; as the scalar τ varies from zero through one, $y(\tau)$traces out the entire line from the observer to the vehicle. The problem is to determine when this ray is tangent to the moon.

The equation of the moon's surface is

$$\left| \bar{y} - \bar{R}_m \right|^2 = a_m^2 \tag{2}$$

where a_m is the radius of the moon. Hence, it is required to find that value of τ for which,

$$\left| \bar{R} + \tau(\bar{x} - \bar{R}) - \bar{R}_m \right|^2 = a_m^2$$

or

$$\left|\bar{R}_m - \bar{R}\right|^2 - 2\tau(\bar{x}-\bar{R})^T(\bar{R}_m - \bar{R}) + \tau^2\left|\bar{x}-\bar{R}\right|^2 = a_m^2 \tag{3}$$

To simplify further work with this equation, introduce the topocentric position (column) vectors,

$$\bar{\psi} = \bar{x} - \bar{R}, \quad \text{position of the vehicle}$$

$$\bar{\gamma} = \bar{R}_m - \bar{R}, \quad \text{position of the moon}$$

and the distance from the observer to the moon's limb,

$$\rho = \left|\bar{R}_m - \bar{R}\right|^2 - a_m^2 \tag{4}$$

Assuming that $\rho > 0$ (i.e., that the observer is outside the moon), equation (3) becomes

$$\left|\bar{\psi}\right|^2 \tau^2 - 2\tau(\bar{\gamma}^T\bar{\psi}) + \rho = 0 \tag{5}$$

This equation will have one root when the ray is tangent to the moon.

Using the discriminant, the requirement for real and equal roots is that,

$$\frac{(\bar{\gamma}^T\bar{\psi})^2}{\left|\bar{\psi}\right|^2} - \rho = 0 \tag{6}$$

or

$$\frac{(\bar{\gamma}^T\bar{\psi})}{\left|\bar{\psi}\right|} = \pm\sqrt{\rho}$$

Since a positive value for τ is desired, and (when the discriminant is zero),

$$\tau = \frac{(\bar{\gamma}^T\bar{\psi})}{|\bar{\psi}|^2} = \pm \frac{\sqrt{\rho}}{|\bar{\psi}|} \tag{7}$$

the positive sign for $\sqrt{\rho}$ is selected. Hence, the ray will be tangent to the moon when the function,

$$\phi = \frac{(\bar{\gamma}^T\bar{\psi})}{|\bar{\psi}|} - \sqrt{\rho} \tag{8}$$

is zero.

This occultation function may be interpreted in terms of projections. In figure 1, the first term of the occultation function is seen to be the projection of $\bar{\gamma}$ on the unit vector, $\bar{\psi}/|\bar{\psi}|$, defining the direction to the vehicle. The second term, $\sqrt{\rho}$, is the magnitude of the distance from the observer to the moon's limb; this length is an element of that cone which is tangent to the moon with apex at the observer. When the projection of $\bar{\gamma}$ on $\bar{\psi}/|\bar{\psi}|$ is equal to $\sqrt{\rho}$, occultation is said to have occurred. Again, in figure 1, whenever the unit vector to the vehicle lies within the cone described above, (between positions 3 and 4, and positions 1 and 2) the projection of $\bar{\gamma}$ on $\psi/|\bar{\psi}|$ will be greater than an element of that cone, and the occultation function will be positive. Conversely, when the unit vector to the vehicle lies outside the cone, the element will be larger than the projection, and ϕ will be negative.

Thus, in one revolution of the satellite, ϕ will be twice positive and twice negative, with four zeros (figure 2). Only those zeros in ϕ for which the satellite is behind the moon (i.e., those corresponding to positions 1 and 2) actually correspond to occultation. The extraneous roots (corresponding to positions 3 and 4) may be identified by testing on $|\bar{\psi}|$, so that this function could be used to predict occultation times. That is, if

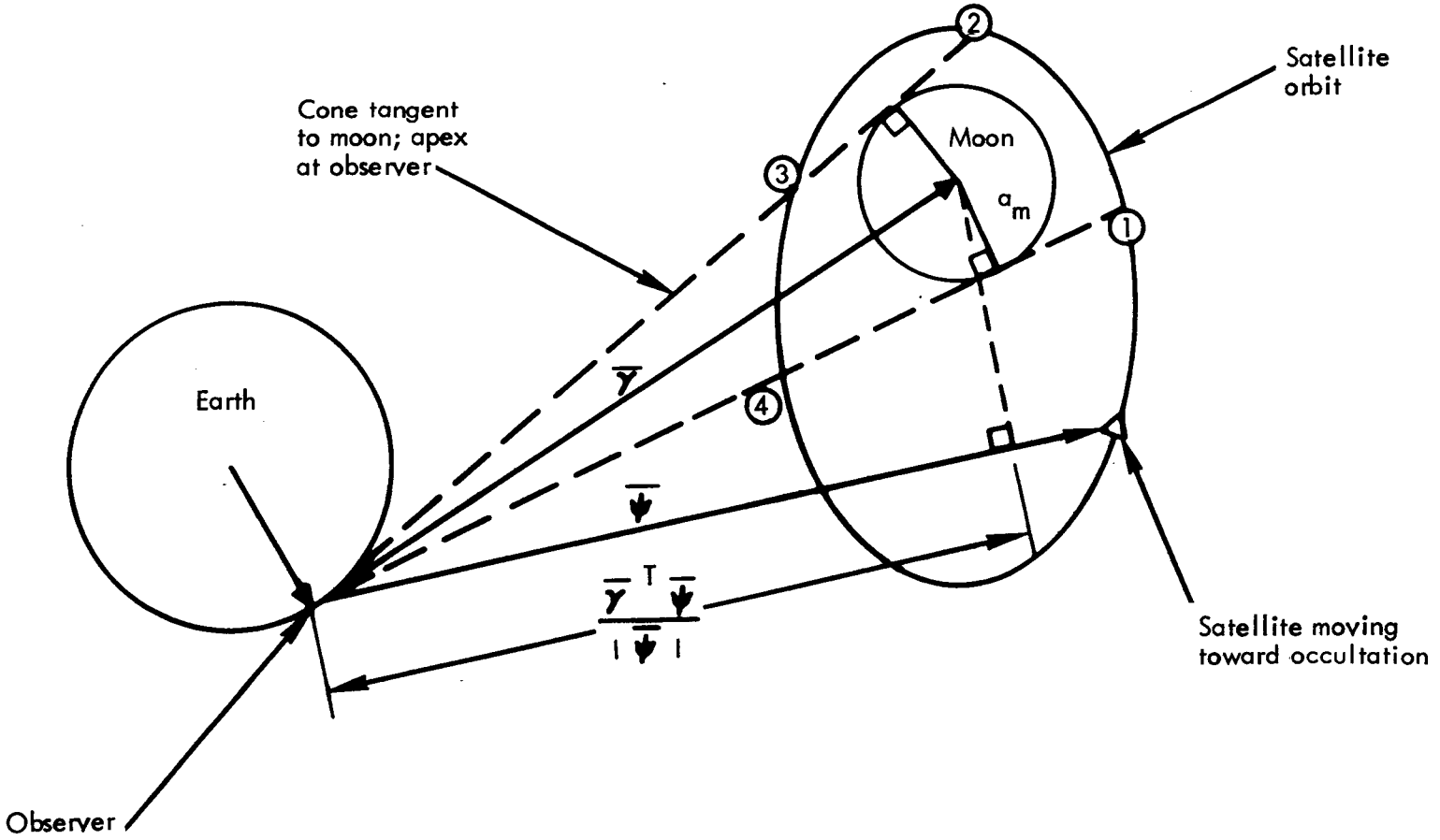

Figure 1.— Geometry of the Earth Occultation Function

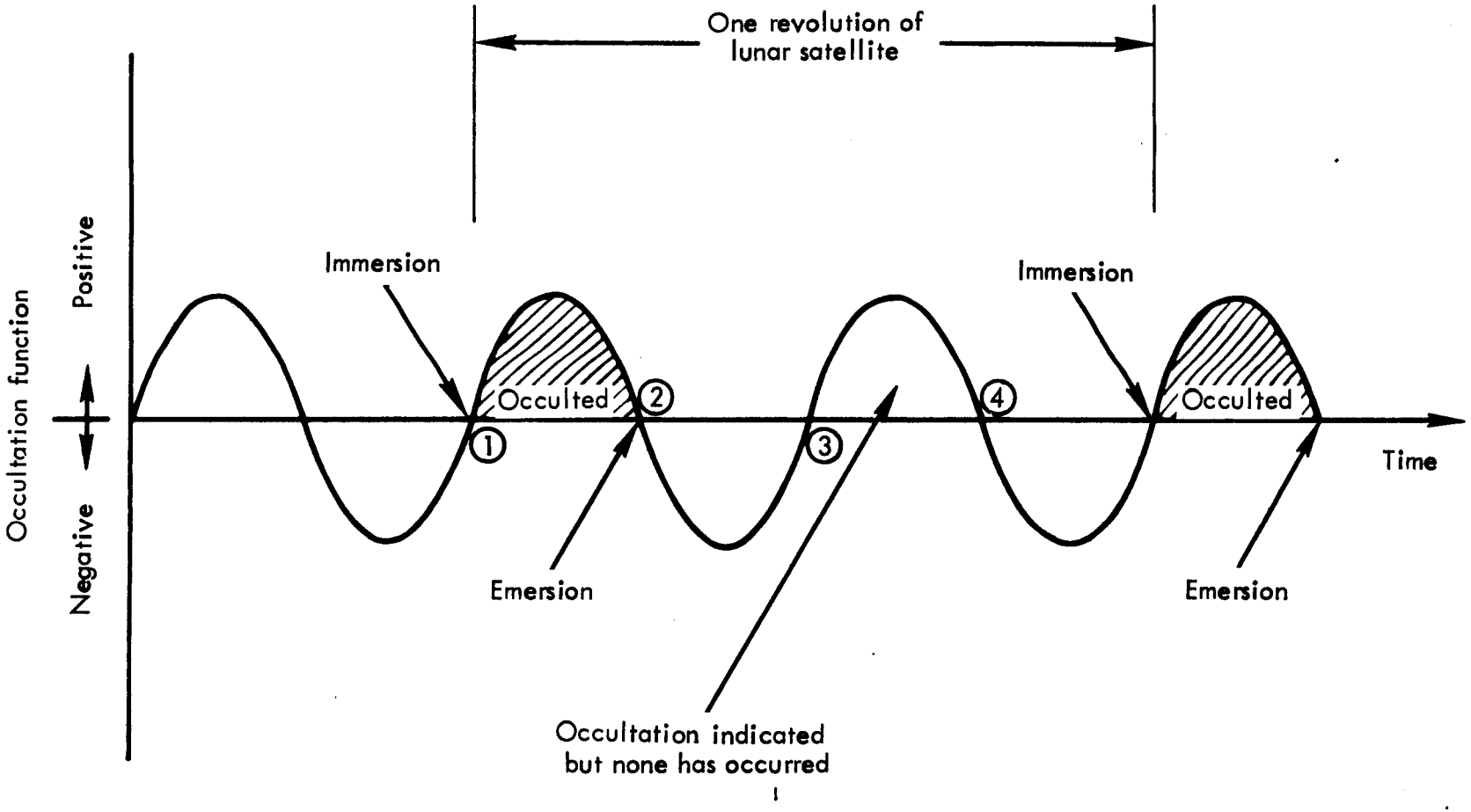

Figure 2.— Time History of the Occultation Function

$|\bar{\psi}| > \sqrt{\rho}$, the satellite is behind the moon;

$|\bar{\psi}| < \sqrt{\rho}$, the satellite is in front of the moon.

Immersion may be distinguished from emersion by noting the sign of the time rate of change of ϕ. In figure 1, as the satellite passes behind the moon (position 1), $d\phi/dt$ is positive; coming out from behind the moon (position 2), $d\phi/dt$ is negative.

For sun occultations, the development of an occultation function is completely analogous to that above, except that $\bar{R}$, the observer's position vector, becomes the geocentric position of the sun.

Certain numerical problems were encountered using this formulation for the sun occultations. The distance to the moon's limb and to the satellite, measured from the sun, are both approximately 2×10^5 earth radii. The subtraction of these two very large and nearly equal lengths in single precision gives no significant figures.

However, the problem was easily solved by interchanging the roles of the vehicle and the observer, and writing a new vector equation, corresponding to equation (1), for the ray from the vehicle to the observer. Introducing the following redefinitions,

$$\bar{\psi} = \bar{R}_s - \bar{x}$$

$$\bar{\gamma} = \bar{R}_m - \bar{x}$$

$$\rho = \left|\bar{R}_m - \bar{x}\right|^2 - a_m^2$$

where $\bar{R}_s$ is the geocentric position vector of the sun, the occultation function may still be computed according to equation (8). With these new definitions for $\bar{\gamma}$ and $\bar{\psi}$, the projection interpretation of ϕ is modified as shown in figure 3. The projection of $\bar{\gamma}$ on $\bar{\psi}/|\bar{\psi}|$, the unit vector in the direction of the observer, is computed. The distance to the moon's limb from the vehicle, ρ, which is an element of the cone tangent to the moon with apex at the vehicle, is subtracted from this projection. Occultation is said to have occurred when this difference is zero. Recall that the function developed for earth occultations had zeros at positions 3 and 4 (figures 1 and 2); evaluating this new occultation function at these points shows that it does not have zeros here, but rather is near its minimum value because the vectors $\bar{\gamma}$ (to the moon) and $\bar{\psi}$ (to the sun) are in opposite directions. For satellite positions between those marked 1 and 2, the occultation function is positive (as was the earlier function). The reason for this apparent disappearance of the two extraneous roots is indicated schematically in figure 4. In both cases the positive $\sqrt{\rho}$ is selected, giving $\tau > 0$, Those positions of the occulting body (in this case, the moon) are shown which give zeros in the occultation function. Note that both functions exhibit two such positions of the occulting body, but for the sun occultation function, only one of them is likely to occur, i.e., it is unlikely for the occulting body to be beyond the observer, as seen from the vehicle. On the other hand, either position of the occulting body is likely to occur for the earth occultation function.

The association of one of these functions with the earth, and the other with the sun was done merely to facilitate discussion. The earth occultations could be handled in exactly the same manner as sun occultations, and, as will be discussed below, if this were to be done in operations there are some very good reasons for so doing.

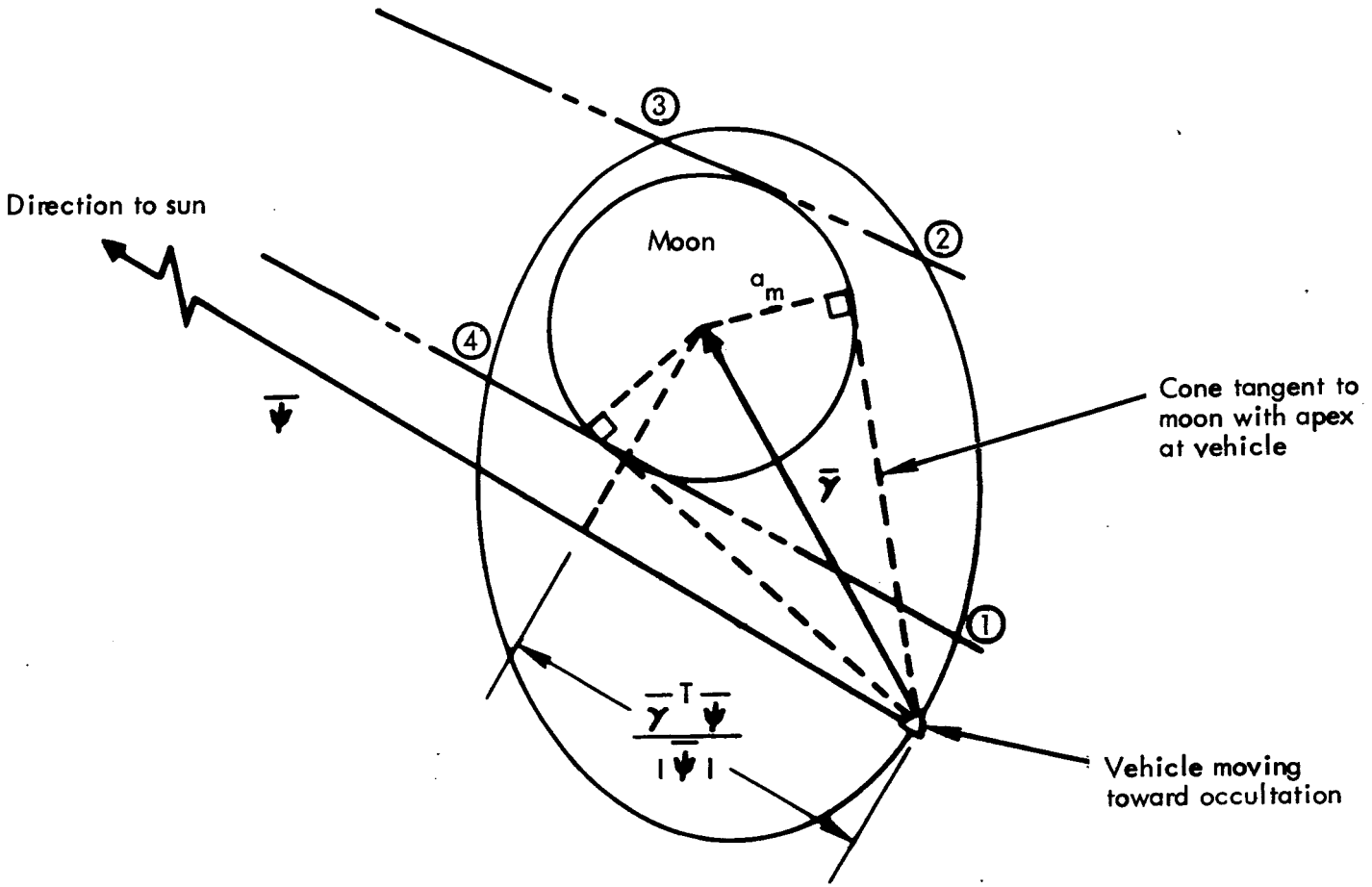

Figure 3.— Geometry of the Sun Occultation Function

Earth occultation function

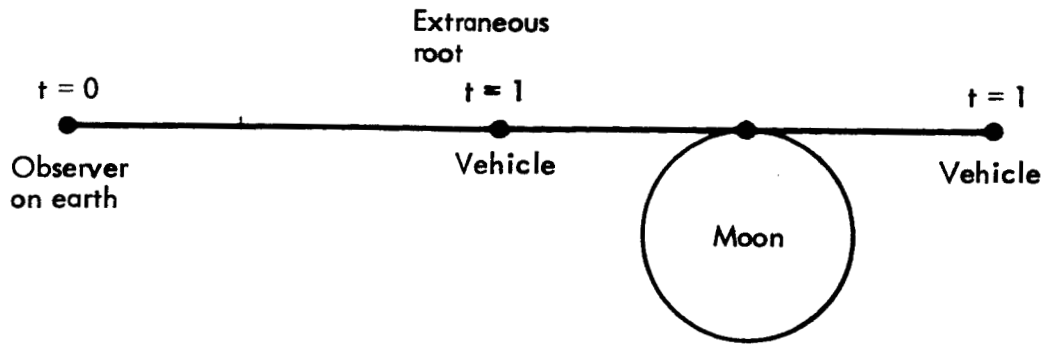

A Equation of ray-observer to vehicle:
$y(t) = \overline{R}_o + t(\overline{x} - \overline{R}_o)$

B Function indicates occultation for either position of the vehicle; both are likely to occur.

Sun occultation function

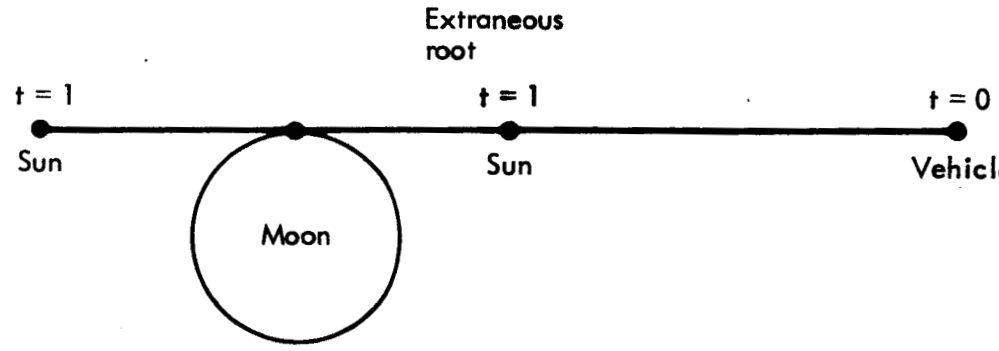

A Equation of ray-vehicle to observer (sun)
$y(t) = \overline{X} + t(\overline{R}_o - \overline{x})$

B Function indicates occultation for either position of the sun. Only position corresponding to actual occultation is likely to occur.

Figure 4.— Occultation Function Comparison

3.2 Differential Correction Program Modifications

In the differential correction process, occultation data are treated in the same manner as any other data type, i.e., the observed minus computed residual in the occultation function is formed, and the partial derivative of the occultation function with respect to the epoch state vector is computed and used to form a row of the normal matrix.

The inputs to the differential correction program consist of occultation times and their standard deviations, σ_t, punched on normal observation cards. The observation cards are blank except for the station ID and the time tag, since the time itself is the observation.

The occultation data processing begins by integrating the equations of motion and the variational equations to the i^{th} observation and noting the data type: If earth occultation, set

$$\bar{R} = \bar{R}_o$$

$$\dot{\bar{R}} = \bar{\omega} \times \bar{R}_o$$

$$\bar{\gamma} = \bar{R}_m - \bar{R}$$

$$\dot{\bar{\gamma}} = \dot{\bar{R}} - \dot{\bar{R}}$$

$$\bar{\psi} = \bar{x} - \bar{R}$$

$$\dot{\bar{\psi}} = \dot{\bar{x}} - \dot{\bar{R}}$$

$$\rho = \bar{\gamma}^T \bar{\gamma} - a_m^2$$

$$\phi = \frac{\bar{\gamma}^T \bar{\psi}}{|\bar{\psi}|} - \sqrt{\rho}$$

$$\frac{\partial \phi}{\partial \bar{x}} = \begin{bmatrix} \phi_x \\ \phi_y \\ \phi_z \\ \phi_{\dot{x}} \\ \phi_{\dot{y}} \\ \phi_{\dot{z}} \end{bmatrix} = \begin{bmatrix} \left[\frac{\bar{\phi}^T}{|\bar{\psi}|} \left(I_{3x3} - \frac{\bar{\psi}\,\bar{\psi}^T}{|\bar{\psi}|^2} \right) \right]_{3x1} \\ \\ \left[0 \right]_{3x1} \end{bmatrix}$$

where

$$\bar{R}_o = \begin{bmatrix} w_1^s \cos \alpha_i \\ w_1^s \sin \alpha_i \\ w_3^s \end{bmatrix}$$

a_m is the radius of the moon, $\bar{x}$ and $\bar{R}_m$ are the geocentric true of date position vectors of the satellite and the moon, respectively, w_j^s are the meridian plane coordinates of the observing station, α_i is the right ascension of the station meridan at time t_i, and $\bar{\omega}$ is the earth's rotational velocity vector.

If sun occultation, set

$$\bar{R} = \bar{R}_s$$

$$\dot{\bar{R}} = \dot{\bar{R}}_s$$

$$\bar{\gamma} = \bar{R}_s - \bar{x}$$

$$\dot{\bar{\gamma}} = \dot{\bar{R}}_s - \dot{\bar{x}}$$

$$\bar{\psi} = \bar{R}_s - \bar{x}$$

$$\dot{\bar{\psi}} = \dot{\bar{R}}_s - \dot{\bar{x}}$$

$$\rho = \bar{\gamma}^T\bar{\gamma} - a_m^2$$

$$\phi = \frac{\bar{\gamma}^T\bar{\psi}}{|\bar{\psi}|} - \sqrt{\rho}$$

$$\frac{\partial\phi}{\partial x} = \begin{bmatrix} \phi_x \\ \phi_y \\ \phi_z \\ \phi_{\dot{x}} \\ \phi_{\dot{y}} \\ \phi_{\dot{z}} \end{bmatrix} = \begin{bmatrix} \left[-\frac{\bar{\psi}}{|\bar{\psi}|} + \frac{\bar{\gamma}}{\sqrt{\rho}} - \left[I_{3x3} - \frac{\bar{\psi}\bar{\psi}^T}{|\bar{\psi}|^2} \right] \frac{\bar{\gamma}}{|\bar{\psi}|} \right]_{3x1} \\ \\ \begin{bmatrix} 0 \end{bmatrix}_{3x1} \end{bmatrix}$$

where $\bar{R}_s$, $\dot{\bar{R}}_s$ are geocentric, true of date position and velocity vectors of the sun, respectively.

Next compute for either type of occultation,

$$\dot{\phi} = \frac{\dot{\bar{\gamma}}^T \bar{\psi}}{|\bar{\psi}|} + \frac{\bar{\gamma}^T}{|\bar{\psi}|}\left[I - \frac{\bar{\psi}\bar{\psi}^T}{|\bar{\psi}|^2}\right]\dot{\bar{\psi}} - \frac{\bar{\gamma}^T\dot{\bar{\gamma}}}{\sqrt{\rho}}$$

$$\sigma_\phi = |\dot{\phi}|\,\sigma_t \,.$$

The residual is then formed at time t_i, by noting that the observed value of the occultation function is zero, i.e., $\phi_{observed} - \phi_{computed} = -\phi_{computed}$.

The row of the normal matrix, a_i, and the contribution to the right hand side of the normal equation, $a_i^T b_i$, are computed,

$$a_i = \frac{\partial\phi}{\partial x_o} = \left(\frac{\partial\phi}{\partial x}\right)^T \frac{\partial x}{\partial x_o}$$

$$a_i^T b_i = -\left(\frac{\partial\phi}{\partial x_o}\right)^T \phi_c$$

where $\partial x/\partial x_o$ is the output of the variational equations integration. The quantities a_i and $a_i^T b_i$ are then divided by σ_ϕ and accumulated into the appropriate matrices in the normal equation.

4. EVALUATION OF OCCULTATION DATA

4.1 Convergence Characteristics

To study the effectiveness of occultation data as an aid to convergence, a series of short data span (about 100 minutes) differential corrections were initiated, using initial conditions which include large energy errors. Range, range-rate, and occultation data were assumed available from the DSN stations at Goldstone, Woomera, and Madrid with range and range-rate measurements taken at the rate of one data set per minute. In all cases, data were simulated for the orbit defined by the following selenographic elements, with epoch equal to the time of pericynthion passage:

$a = 3732.6$

$e = .455$

$i = 15.0$

$\ell = 25.46$

$\omega = 347.54$

$T = 27$ June 1966, $4^h0^m48^s$

Period = 340 min

The estimate of the initial conditions used to start the differential correction was based on a nominal LOPP state vector defined by the following selenographic elements:

$a = 2788$ km

$e = 0.2869$

$i = 15.0$

$\Omega = 25.47$

$\omega = -12.46$

$T = 27$ June 1966, $4^h0^m48^s$

Period = 220 min

The geocentric and heliocentric occultation times for Goldstone, Woomera, and Madrid are listed in Table I.

TABLE I

OCCULTATION TIMES FOR THE OBSERVED ORBIT

Time measured from epoch 27 June 1966, $4^h0^m48^s$		
	Immersion	Emersion
A) Geocentric		
Goldstone	$5^h51^m4^s$	$7^h17^m46^s$
	$23^h16^m59^s$	$0^h29^m48^s$ (28 June)
Woomera	$5^h51^m46^s$	$7^h19^m22^s$
	$11^h37^m51^s$	$13^h5^m27^s$
Madrid	$17^h28^m37^s$	$18^h56^m33^s$
	$23^h14^m44^s$	$0^h26^m14^s$ (28 June)
B) Heliocentric		
Station Independent	$8^h10^m22^s$	$9^h8^m24^s$
	$13^h51^m34^s$	$14^h49^m42^s$

The occultation patterns for this orbit is discussed in more detail in reference 2.

It was found that as the weights on the occultation data were increased (i.e., as their standard deviations were decreased), convergence became slower, and finally was not achieved at all. These poor convergence characteristics can be attributed to the inconsistent residual problem which was discussed in reference 2. Because of the large energy error, the computed position of the spacecraft may correspond to an emersion point, while the spacecraft is actually just passing behind the moon (immerging). The residual would then be small, because the computed vehicle is conincidentally near an extraneous zero in the occultation function. Differential correction based on this residual is

obviously meaningless, since an emersion time has been paired with an immersion time. This is illustrated in figures 5 and 6, which present the time histories of the occultation function and its time derivative for earth occultations as viewed from the DSN station at Goldstone. In figure 5 the first occultation occurs at Goldstone at approximately 110 minutes from epoch. The ϕ residual is already large, and the sign of $d\phi/dt$ (figure 6) is incorrect. The second occultation occurs at approximately 200 minutes from epoch, as the satellite comes out from behind the moon. Here the residual is very small, calling for essentially no correction to the epoch state vector; yet there is a substantial energy error, since an observed emersion time has been paired with a computed immersion time. Figure 6 indicates how the time histories of $d\phi/dt$ get completely out of phase in a single revolution of the observed satellite.

This problem will show up with any periodic data type; however, the fact that the earth occultation function has four zeros per revolution, while range, and range-rate have only two, accounts for the much greater sensitivity of earth occultation data to energy errors. The same phenomenon will appear in most formulations designed to allow usage of occultation data; for example, the Orbit Determination Program (ODP) of the Jet Propulsion Laboratory (reference 3), which uses the observed occultation time and differences in certain topocentric angles to compute residuals, will be subject to the same restrictions.

The difficulty can be removed by using the function developed for sun occultation for both data types; occultation data will at least then be no worse than, say, range or range-rate data in its sensitivity to energy errors. In the JPL ODP mentioned above, the rule of interchanging the observer and the vehicle will also eliminate the extraneous zeros.

The same set of cases (with σ_t as a parameter) were re-run with much smaller errors in the initial conditions. The purpose was to determine if occultation data are an aid to convergence, given consistent and meaningful residuals. Figures 7 and 8 present the iteration histories for differential corrections using four occultation data qualities, with the percentage of the required state vector correction attained plotted against iteration number;

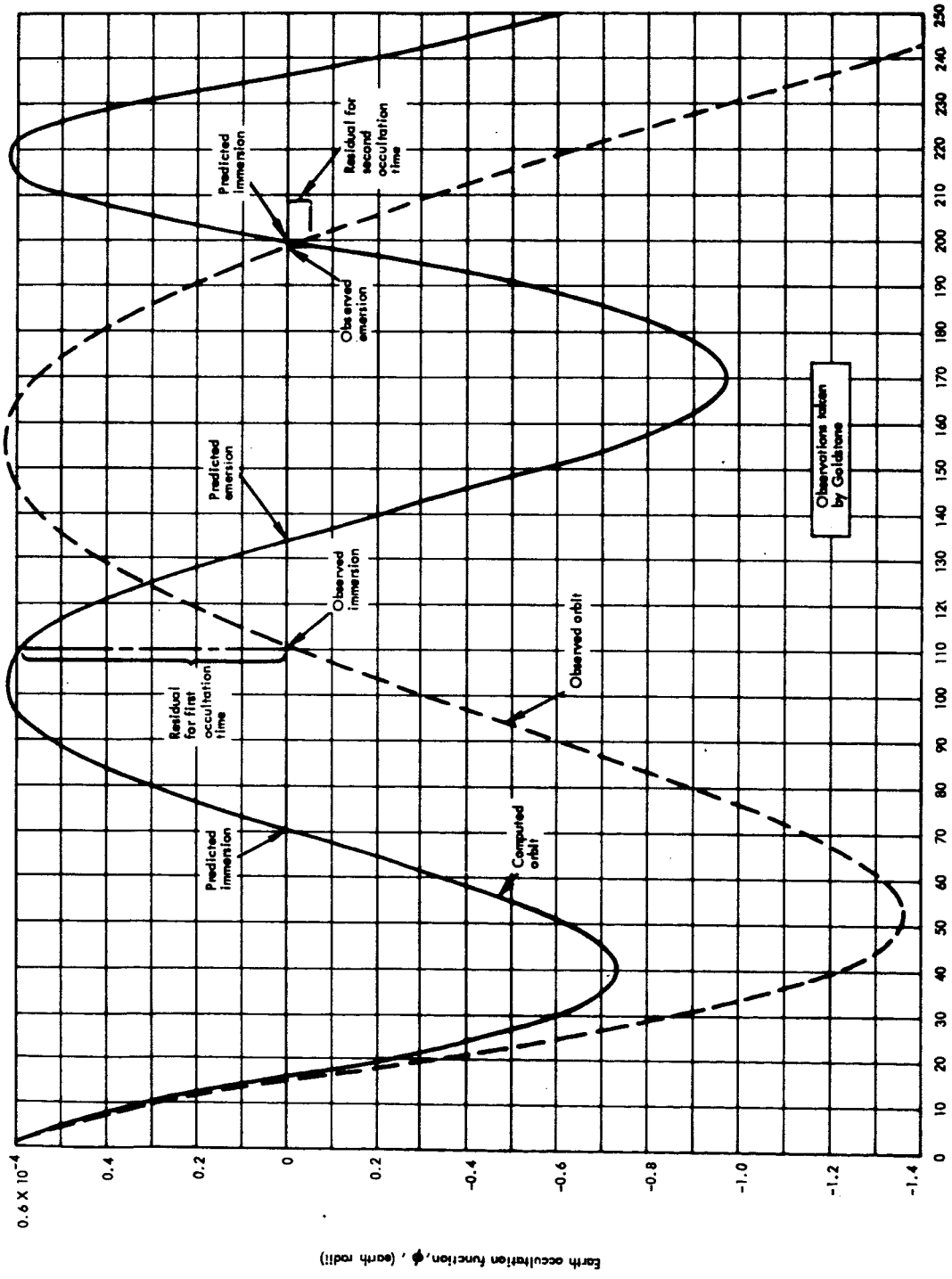

Figure 5.— Earth Occultation Function Time History

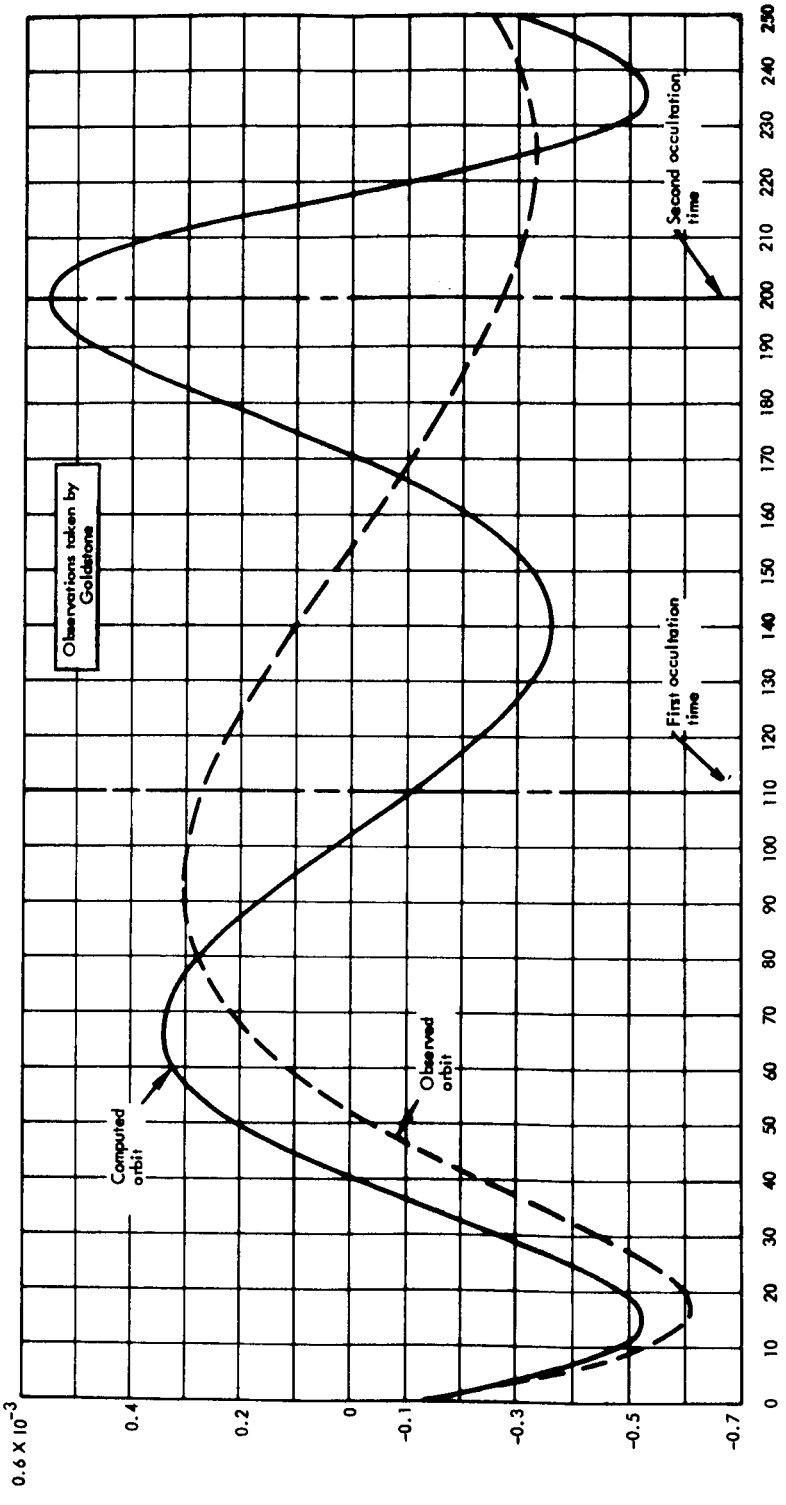

Figure 6.— Derivative of the Earth Occultation Function

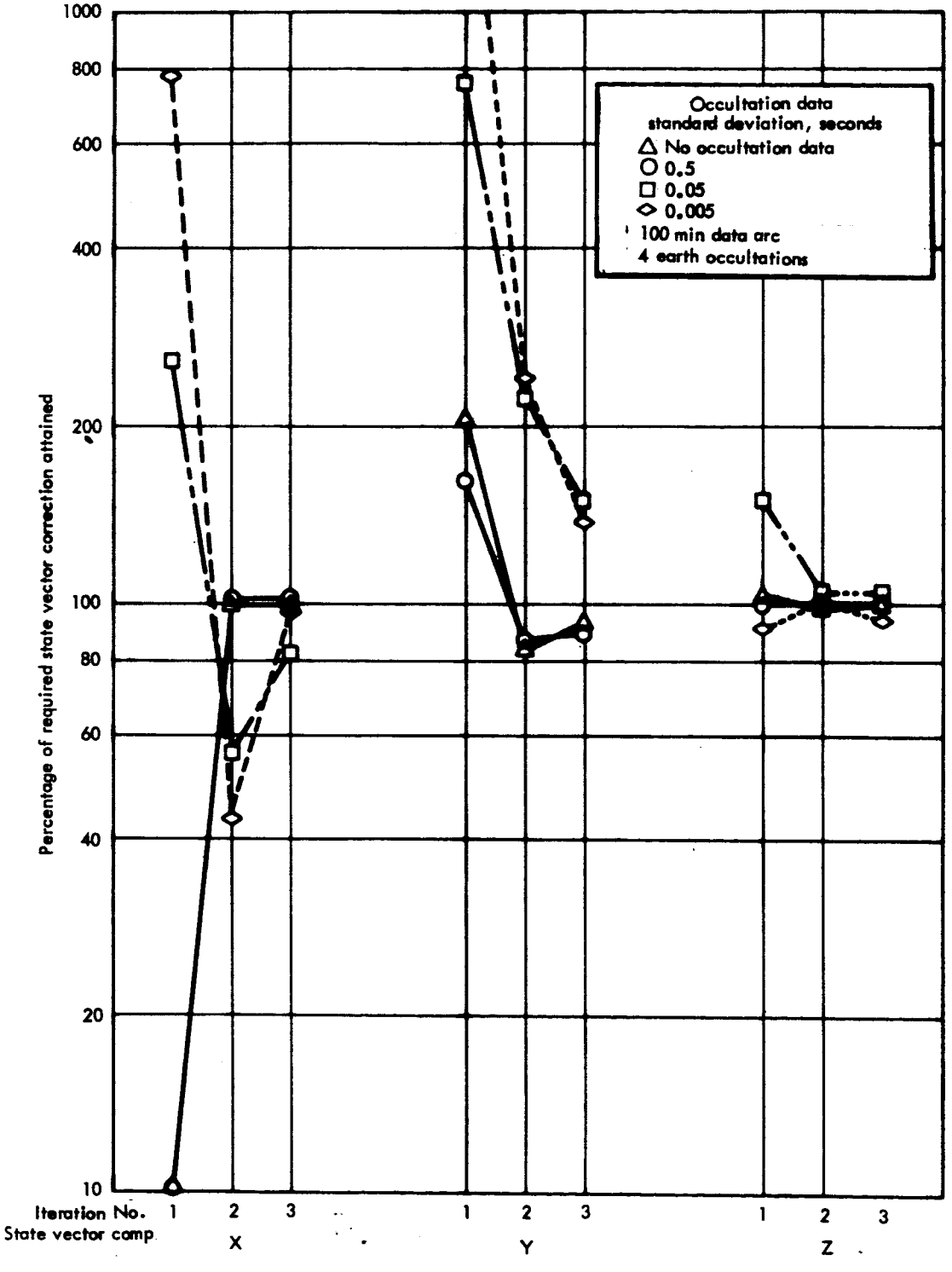

Figure 7.— Effect of Occultation Data on Convergence — Position Components

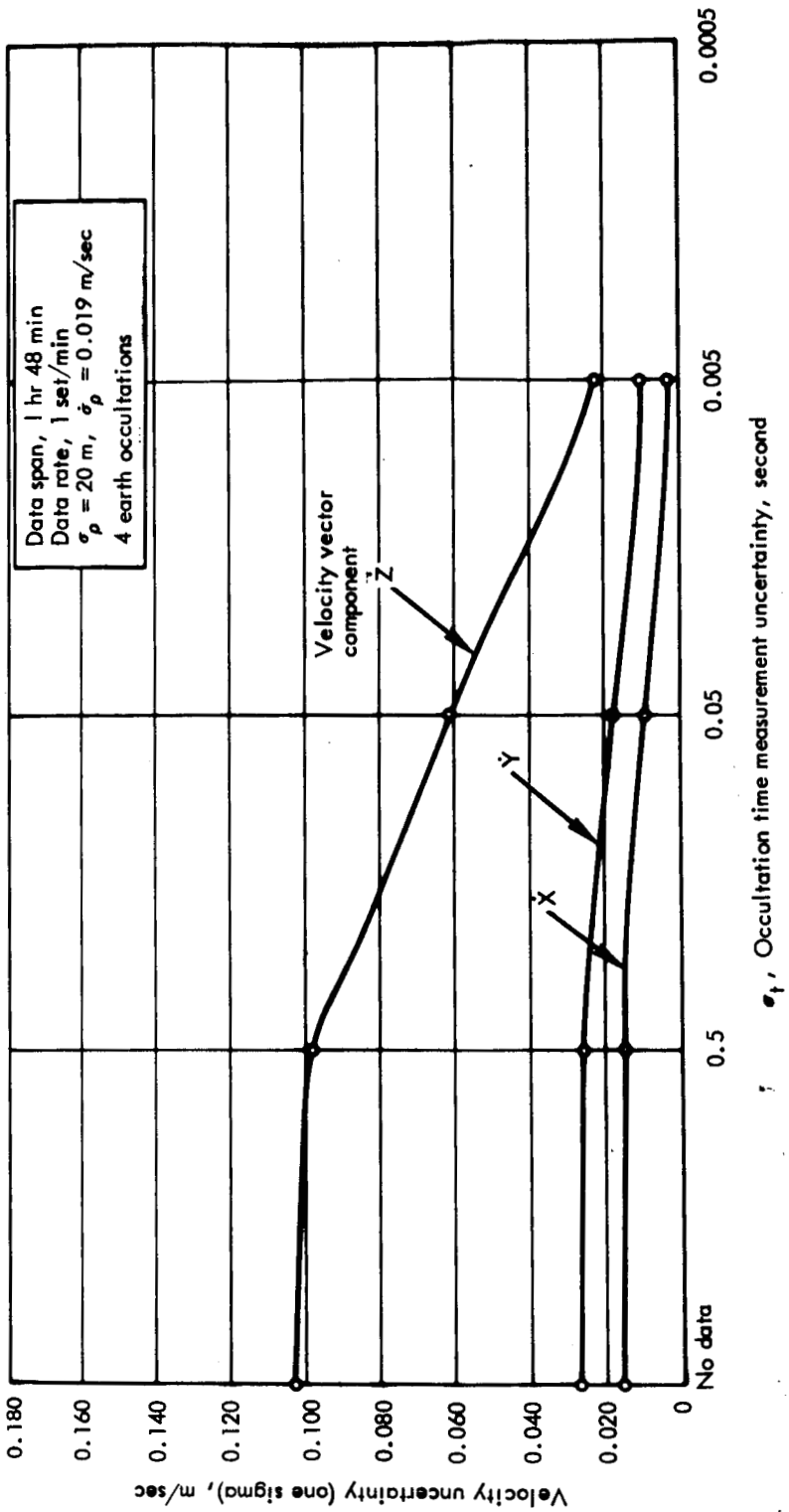

Figure 8.— Effect of Occultation Data on Convergence — Velocity Components

position components are presented in figure 7, velocity components in figure 8. In almost all cases, adding occultation data slowed convergence, with the higher quality data (σ_t = .005 second) having the most serious effect.

The effect occultation data has on convergence is, of course, strongly influenced by the sensitivity of the epoch state vector to changes in the occultation function.

If the earth occultation function used here were replaced by the sun occultation function (as has been suggested above, to eliminate extraneous zeros), the partial derivative, $\partial\phi/\partial x$, may exhibit different convergence characteristics.

4.2 Reduction of State Vector Uncertainties

The uncertainties in the converged state vector as a function of the occultation time measurement uncertainties, are presented in figures 9 (position components) and 10 (velocity components). Note that the nominal occultation data quality has a negligible effect when used with the one per minute range, range-rate data rate. However, a one order-of-magnitude improvement in the quality of the occultation data reduces the uncertainties to roughly half their former values.

The effect of bias in the occultation data was investigated by running two short arc fits to convergence, with and without a 3-second bias in the occultation data. The converged state vectors for these two cases differed by less than 100 meters in position components and by less than 0.1 m/sec in the velocity components. The uncertainties in the converged result differed by less than 0.3 m in position and 10^{-5} m/sec in velocity. Apparently, a bias of this size causes no significant degradation in the quality of the converged result.

The utility of the nominal occultation data (σ_t = 0.5 and 0.7 second) for a reduced data rate was studied by using one $\rho, \dot{\rho}$ set per 10 minutes from the DSN stations. The resulting uncertainties are presented in table II for both

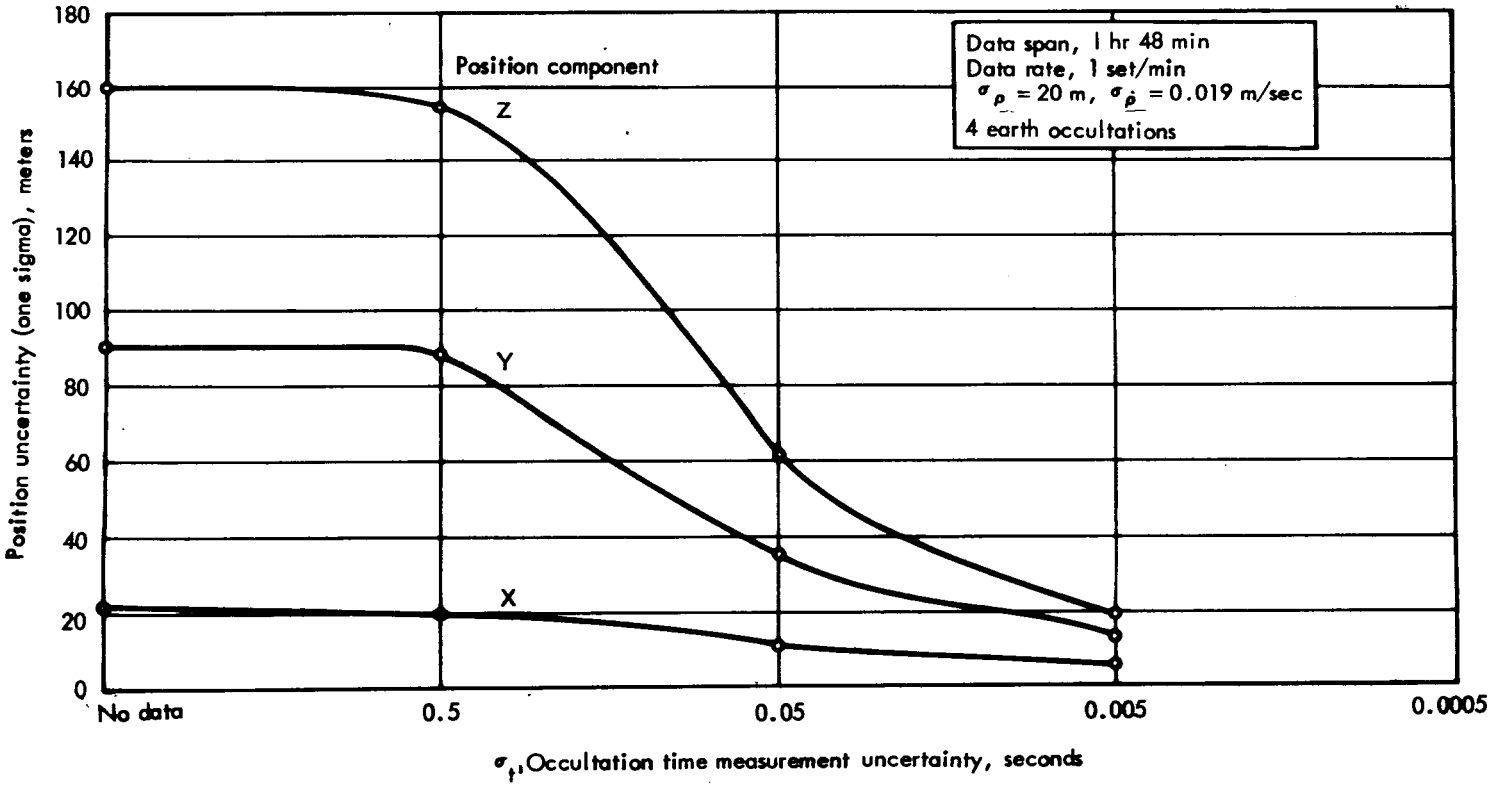

Figure 9.— Effect of Occultation Data on State Vector Uncertainties — Position Components

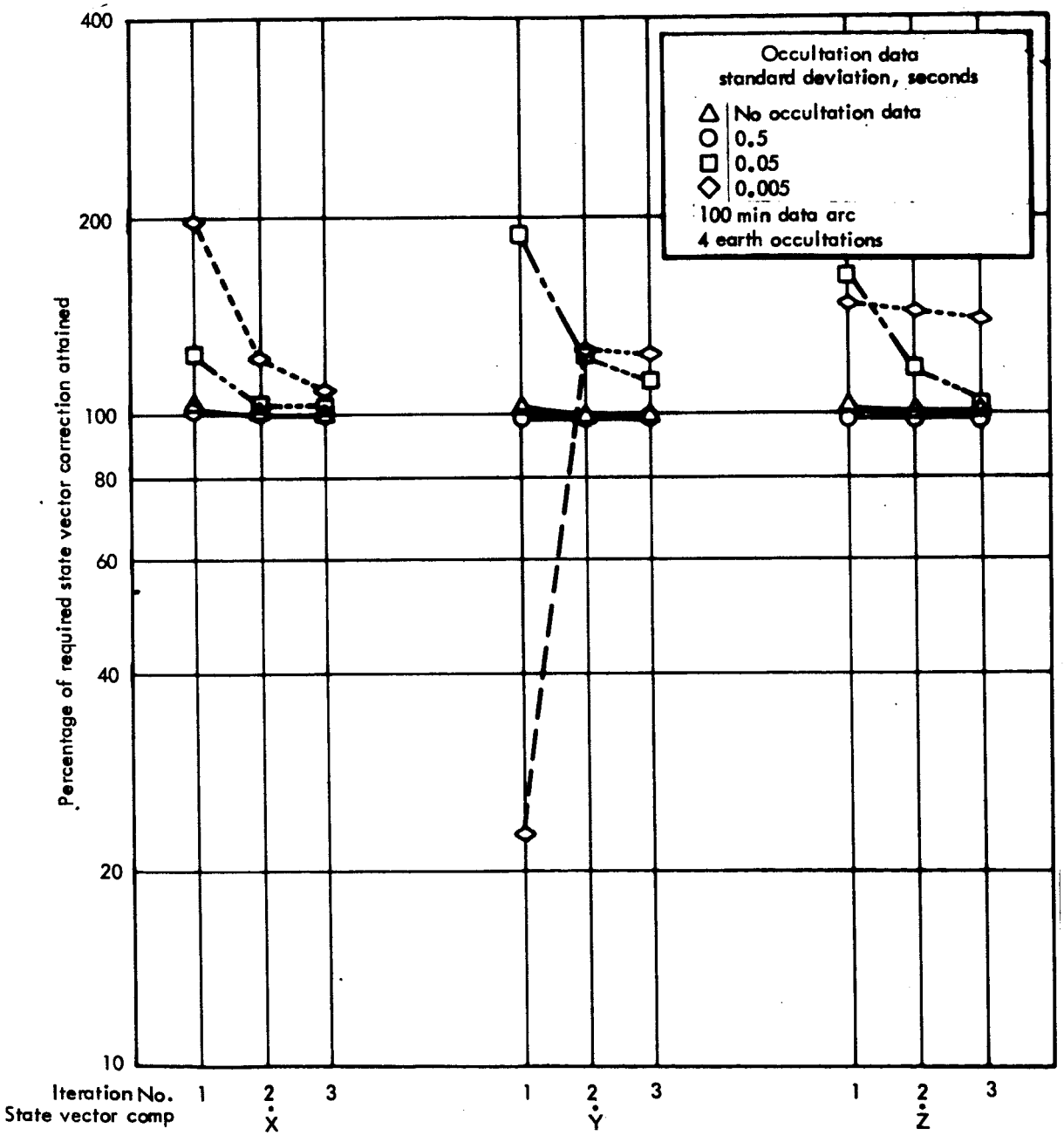

Figure 10.— Effect of Occultation Data on State Vector Uncertainties — Velocity Components

TABLE II

EFFECT OF OCCULTATION DATA USING A REDUCED $\rho,\dot{\rho}$ DATA RATE

AEP3 orbit; data rate, 1 $\rho,\dot{\rho}$ set per 10 min; σ_t = 0.5 sec earth occultations; 0.7 sec sun occultations; Position uncertainties in km; Velocity in m/s;

A) 1-Hour 48-Minute Data Arc

State vector component	Uncertainties (one sigma)	
	24 $\rho,\dot{\rho}$ observations	Four earth occultation times plus 24 $\rho,\dot{\rho}$ observations
x	.04825	.04249
y	.22165	.18709
z	.39292	.33059
$\dot{x}$	.07	.06
$\dot{y}$	.28	.25
$\dot{z}$	.41	.37

B) 6-Hour Data Arc

State vector component	Uncertainties (one sigma)	
	78 $\rho,\dot{\rho}$ observations	Four earth occultation times plus 78 ρ, $\dot{\rho}$ observations
x	.01871	.01862
y	.04270	.04240
z	.05398	.05349
$\dot{x}$	.025	.024
$\dot{y}$	.096	.091
$\dot{z}$	.141	.133

short (1 hour) and long (6 hour) data spans. The first column is a list of state vector uncertainties when only $\rho, \dot{\rho}$ data are used (a total of 24 data points). Listed in the second column are the uncertainties which result when occultation data (four earth occultations) are added to the range, range-rate data. For the 6-hour data arc, the occultation data have an insignificant effect. Note however, that still only four occultation observations have been used. Extending the data arc another 1-1/2 hours would include an additional two occultations, which would reduce the uncertainties more than shown in table II.

For very short data arcs (less than 15 minutes), the addition of nominal quality occultation data was found to be very effective. The results are presented in table III for 5-, 10-, and 15-minute data arcs; in every case, the uncertainties in the velocity components are reduced by one order of magnitude or more. Thus, occultation data may be of considerable value for a mission in which the vehicle passes behind the moon shortly after being injected into a selenocentric orbit.

TABLE III

EFFECT OF OCCULTATION DATA WITH VERY SHORT DATA ARCS

AEP3 orbit; data rate, 1 $\rho, \dot{\rho}$ set per min;
σ_t = 0.5 sec earth occultations, immersion only used; Position uncertainties in km; Velocity in m/s.

A) 5-Minute Data Arc

State vector component	Uncertainties (one sigma)	
	24 $\rho, \dot{\rho}$ observations	Two earth occultation times plus 24 $\rho, \dot{\rho}$ observations
x	.437	.340
y	.694	.547
z	.914	.730
$\dot{x}$	7.33	.29
$\dot{y}$	10.74	.48
$\dot{z}$	14.53	.62

TABLE III. - Concluded

EFFECT OF OCCULTATION DATA WITH VERY SHORT DATA ARCS

AEP3 orbit; data rate, 1 $\rho,\dot{\rho}$ set per min;
σ_t = 0.5 sec earth occultations, immersion
only used; Position uncertainties in km;
Velocity in m/s.

B) 10-Minute Data Arc

State vector component	Uncertainties (one sigma)	
	44 $\rho,\dot{\rho}$ observations	Two earth occultation times plus 24 $\rho,\dot{\rho}$ observations
x	.332	.167
y	.515	.298
z	.695	.399
$\dot{x}$	1.73	.16
$\dot{y}$	2.53	.28
$\dot{z}$	3.45	.37

C) 15-Minute Data Arc

State vector component	Uncertainties (one sigma)	
	64 $\rho,\dot{\rho}$ observations	Two earth occultation times plus 64 $\rho,\dot{\rho}$ observations
x	.234	.120
y	.372	.228
z	.504	.306
$\dot{x}$	.72	.13
$\dot{y}$	1.05	.23
$\dot{z}$	1.44	.30

5. CONCLUSIONS AND RECOMMENDATIONS

With the current formulation, occultation data will not aid convergence, because of the inconsistent residual problem. Interchanging the vehicle and observer will give occultation residuals no more sensitive to energy errors than those of range and range-rate observations. However, even with consistent residuals, occultation data does not appear to be a useful aid to covergence when used with $\rho,\dot{\rho}$ data arcs of more than 1 hour.

The occultation data of nominal quality, when used in conjunction with range and range-rate data taken from the DSN stations at the rate of one set per minute, reduces the uncertainties in the converged result only slightly. However, decreasing the occultation uncertainties one order of magnitude gives uncertainties roughly half what they are using range and range-rate only.

Further study should include formulation of the earth occultation function with the vehicle and observer interchanged to eliminate the extraneous zeros. Alternate forms of the occultation function might also be studied, including the function consisting of a comparison of the moon's radius with the shorter leg of the projection triangle of figure 1. Particular emphasis should be placed on the sensitivity of these alternate forms to changes in the epoch state vector and consequently in their effect on the convergence of the differential correction process.

Finally, a more detailed comparison of the relative usefulness of earth, sun, and star occultations would be appropriate, perhaps not so much for the LOPP mission as for Apollo, where a large number of occultations could be observed from onboard the spacecraft.

6. NEW TECHNOLOGY

This section is included to comply with the requirements of the "New Technology" clause of the Master Agreement under which this report was prepared. Described herein are the results of a study of the effectiveness of occultation data in differential correction. The most significant new technology is the exposing of extraneous zeros (and corresponding inappropriate application) in existing mathematical functions which are used for differential correction with occultation data. Methods of bypassing the difficulty are indicated.

REFERENCES

1. Morrison, D.D.: An Occultation Function for Use in Differential Correction. Memo 9883.4-19, TRW Systems, TRW Inc., Jan. 5, 1966.

2. Lewis, D.H.; Lavoie, P.A.; and Ingram, D.S.: Differential Correction and Preliminary Orbit Determination for Lunar Satellites. NASA CR-66038, Dec. 1, 1965.

3. Warner, M.R., et al: The Orbit Determination Program of the Jet Propulsion Laboratory. Rep. TM 33-168, Jet Propulsion Laboratory, Mar. 18, 1964.